

NUMERICAL SIMULATION OF O₃ AND NO REACTING IN A TUBULAR FLOW REACTOR

Norbert J. Modliński, Włodzimierz K. Kordylewski, Maciej P. Jakubiak

Wroclaw University of Technology, Institute of Heat Engineering and Fluid Mechanics, Wybrzeże
Wyspiańskiego 27, 50-370 Wroclaw, Poland

A process capable of NO_x control by ozone injection gained wide attention as a possible alternative to proven post combustion technologies such as selective catalytic (and non-catalytic) reduction. The purpose of the work was to develop a numerical model of NO oxidation with O₃ that would be capable of providing guidelines for process optimisation during different design stages. A Computational Fluid Dynamics code was used to simulate turbulent reacting flow. In order to reduce computation expense a 11-step global NO - O₃ reaction mechanism was implemented into the code. Model performance was verified by the experiment in a tubular flow reactor for two injection nozzle configurations and for two O₃/NO ratios of molar fluxes. The objective of this work was to estimate the applicability of a simplified homogeneous reaction mechanism in reactive turbulent flow simulation. Quantitative conformity was not completely satisfying for all examined cases, but the final effect of NO oxidation was predicted correctly at the reactor outlet.

Keywords: numerical modelling, global mechanism, de-NO_x, nitric oxide, ozonation

1. INTRODUCTION

Pre-oxidising absorption methods are an alternative to other post combustion treatment technologies of NO_x emission control from coal-fired power plants. These are based on the oxidation of practically insoluble nitric oxide to soluble higher nitrogen oxides and their removal from the flue gas in wet scrubbers (Cooper et al., 1994; Dora et al., 2009; Ellison et al., 2003). The oxidising stage is necessary because flue gas released from coal-fired power plants contains mainly NO (NO₂ is only approx. 5% of all NO_x).

Several strong oxidants (O₃, ClO₂, NaClO or H₂O₂) could be used to transform NO into higher nitrogen oxides (Chironna and Altshuler 1999). One of the most efficient and promising substances from the practical point of view is ozone (Jakubiak and Kordylewski, 2010; Prather and Logan, 1994; Wang et al., 2007). However, its characteristic feature is a relatively short life-time, especially at elevated temperatures. Therefore the performance of NO oxidation with ozone is important, because NO_x cannot be effectively captured in an absorber without conversion of NO into higher oxides. Currently numerous publications describing chemical process of nitrogen monoxide oxidation with ozone are available (Jakubiak and Kordylewski, 2011; Jaroszyńska-Wolińska, 2009; Mok and Lee, 2006; Nelo et al., 1997; Puri, 1995; Skalska et al., 2011; Wang et al., 2006).

Commercialisation of this method has met some economic obstacles, mainly because ozone production is expensive due to oxygen demand and high energy consumption (Jakubiak and Kordylewski, 2012). Further studies are necessary in order to reduce the costs of ozonation by optimisation of ozone use. An

*Corresponding author, e-mail: norbert.modlinski@pwr.wroc.pl

engineering tool capable of predicting NO oxidation with O₃ would be very helpful in optimising the process during the design stage.

For practical as well as mathematical reasons, one of the possible approaches to describe chemically reacting flow situations would be to employ idealised models of reduced dimensionality (Kee et al., 2003). A parametric investigation of low-temperature NO oxidation with O₃ was conducted using a Perfectly Stirred Reactor (PSR) in (Puri, 1995). A 69-step reaction mechanism was employed but no experimental verification was shown. A PSR was used to study ozonising chamber for the oxidation of NO (Mok and Lee, 2006). Computations performed with a selected 11-step global mechanism agreed well with the experimental data.

In case of a tube flow one-dimensional plug-flow reactor could be considered. However, the model should be sensitive to different transport-related phenomena, e.g. flow arrangement and aerodynamics, ozone injection pattern, mixing of reactants, residence time in any complex three-dimensional geometry of the possible reaction channel. To calculate O₃ – NO reaction co-flow and counter-flow turbulent jets Computational Fluid Dynamics needs to be incorporated, since it is better able to account for geometric complexity, at the expense of being more limited in its treatment of the underlying chemistry of the reactive process being studied.

Numerical methods have found wide applications for simulating reactive flow and heat exchange processes (Smoot, 1993). Turbulence – chemistry interaction models are generally used to investigate combustion phenomena. The current paper incorporates an Eddy Dissipation Concept (EDC) (Magnussen, 1981) to describe finite-rate chemistry of NO ozonation.

The work is quite unique since to the best of the authors' knowledge it is one of a few describing reactive turbulent flow with NO ozonation. In (Mok and Lee, 2006) the Direct Numerical Simulation method was applied to simulate ozone injection technology for NO_x control. DNS is the most precise numerical method and a useful tool in fundamental research of turbulence and reactive flow. Unfortunately it is extremely computationally expensive. The authors used a 20-species, 65-step detailed kinetic mechanism between ozone and NO_x. CPU and memory limitations prohibit implementation of such an approach into CFD simulations of practical engineering problems. It is necessary to evaluate the performance of a traditional turbulence model with a simplified global reaction mechanism that approximates real chemical reactions in terms of major species.

In the current paper a turbulence modelling approach with a global 11-step kinetic mechanism that can represent important aspects of detailed mechanism behaviour was employed. The results of numerical modelling versus the measurement data obtained from the experimental apparatus were presented. The investigations were conducted in a tubular flow reactor which could imitate the flue gas channel in a coal fired-power plant. It was demonstrated that the developed numerical model of NO/O₃ chemical reactions in turbulent flows is helpful in predicting effectiveness of nitric oxide ozonation depending on the reactor geometry and the ozone injection pattern.

2. EXPERIMENTAL SETUP

Experimental research was carried out in the laboratory apparatus presented in details in previous studies (Jakubiak and Kordylewski, 2011). The oxidation flow reactor was made from a Plexiglas tube of the inner diameter $D = 60$ mm and the length $L = 2$ m. In order to provide uniform flow velocity profile and generate turbulence a steel grid with the mesh 0.5×0.5 mm was installed at the inlet of the reactor. Along the reactor's axis there were 12 measurement locations in the wall through which a probe was inserted for aspiration of gas samples into the gas analyser. The distance between the measurement locations was 10 cm (Fig. 1).

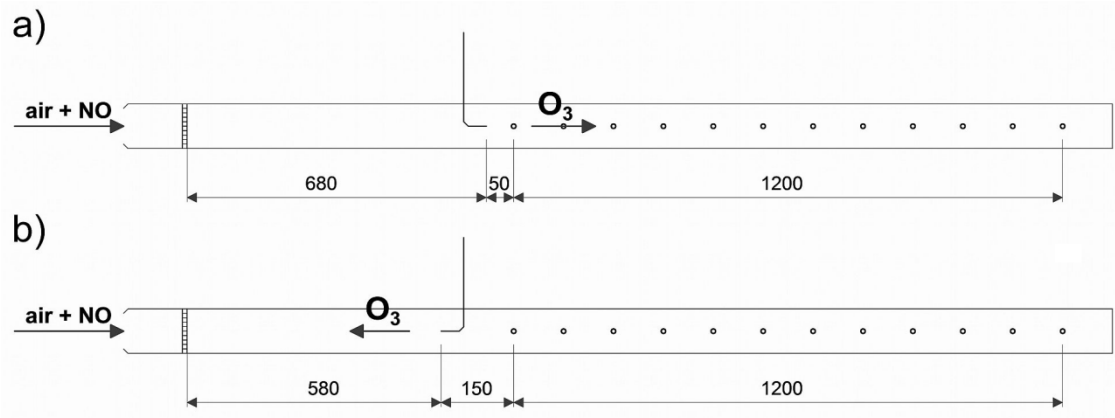


Fig. 1. Measurement locations in the reactor a) co-current injection, b) counter-current injection

Air was the carrier gas for NO/N_2 mixture. It was supplied by the compressor equipped with dryer. The moisture content was far below saturation. The initial mole fraction of NO was kept constant at 100 ppm. Ozone ($32\div 48$ g of O_3 per m^3 of oxygen) was injected in a co- and counter-current pattern into the carrier gas by a single nozzle located in the reactor's axis (inner diameter of the nozzle was $D = 0.52$ mm). The mole fractions of NO and NO_2 in the carrier gas were measured by aspirating gas samples at selected sites into the gas analyser.

The experiment was performed at atmospheric pressure and ambient temperature of 20 °C. The electrochemical sensors of the gas analyser were protected against the residual ozone by a thermal destructor of ozone working at 175 °C. It must be emphasized that NO does not react with O_2 in this temperature range and NO_2 would not undergo destruction to NO in temperatures lower than 1200 °C. Experimental data of NO_x concentrations are not affected by the temperature of ozone destructor. Boundary conditions of the experiment are shown in Table 1.

Table 1. Process parameters of the experiment

Parameter	Unit	Value
Process temperature	°C	20
Volumetric flow rate of the carrier gas (air)	m^3/h	20
Initial mole fraction of NO	ppm	100
Initial mole fraction of NO_2	ppm	5 ± 2
Volumetric inflow rate of oxygen + ozone into the oxidising reactor	dm^3/h	135
Concentration of ozone in oxygen	g/m^3	32, 48
Ratio of molar fluxes, $X = [O_3]/[NO_{ref}]$	$(mol/s)/(mol/s)$	1.0, 1.5
Temperature of the ozone destructor	°C	175

3. NUMERICAL MODEL

3.1. General fluid dynamics

Reducing a complex physical problem to a series of models that can be solved numerically requires a number of assumptions to be made. Specifically for engineering problems momentum and species transport equations must be modelled. Simulations are computed using the commercial CFD code

Fluent, which solves Reynolds averaged Navier-Stokes equations using a low order finite volume formulation. In the current work, the steady-state solution is calculated using second-order discretisation for all equations.

The pressure interpolation was set to PRESTO (Pressure staggering) and Pressure-Velocity coupling was achieved with the SIMPLEC-based algorithm (Van Doormaal and Raithby, 1984) using an unstructured grid, in which an equation for pressure correction is derived from the continuity equation.

The Reynolds Stress Model (RSM) (Launder et al., 1975) solving 5 stress transport equations and equations of turbulent kinetics energy transport and the dissipation rate of turbulent kinetic energy was used as a closure of turbulent Reynolds equations. Predictive performance of RSM is much more accurate compared to eddy-viscosity models in situations where sudden changes in the strain rate occur (e.g. counter-flow jets).

The 3-D tubular reactor geometry can be reduced to 2-D axial-symmetric problem. The computational grid was composed of 50 thousands control volumes.

Boundary conditions are discussed below. Inlet: experimental data at the entry are used. Outlet: it is assumed that in case of the exit plane normal to the axis (x) direction, the axial gradients of all variables except axial velocity are zero. Values of axial velocity at the exit are initially assumed to be the same as those immediately upstream of the exit plane and subsequently scaled appropriately to satisfy overall mass conservation. Hence, at the exit plane it may be written as $(\partial\phi/\partial x)_{\text{exit}} = 0$. Axis of symmetry: at the axis of symmetry, the radial and tangential components of velocity, and radial gradients of other variables are set to zero. Wall: At a wall, no slip condition is applied and the values of velocity components are set to zero. The flow near the wall is influenced by molecular viscosity rather than by turbulence. The wall function method of (Launder and Spalding, 1974) which uses algebraic formulations to link quantities at the wall to those further away.

Due to either a tiny injection diameter of ozone inlet, the nozzle in the carrier gas was simulated numerically as an additional source term in the transport equations of mass, momentum, energy, turbulent kinetic energy, rate of turbulent kinetic energy dissipation and species concentrations in the control volume corresponding to the injection location.

3.2. Gas phase reaction

Both the chemical kinetics and the interaction between turbulence and chemical reactions involved have to be modelled accurately to predict ozonation. The addition of a large number of chemical species complicates turbulent reaction modelling since chemical reaction rates depend non-linearly on species concentrations (Warnatz et al., 2006). Fast chemistry assumption is often made for turbulent reacting flow. This means that turbulent motions control the reaction rate, and hence simplify the description of the reacting flow to that of a mixing problem (Spalding, 1976). The assumption of fast chemistry may be invalid in case of $\text{O}_3 - \text{NO}$ reaction. It is also not recommended for multistep mechanisms with significantly different reaction rates.

More elaborate models also take into account finite-rate chemistry, for example the Eddy Dissipation Concept (EDC) by Magnussen (1981). The EDC model includes detailed chemical mechanisms in turbulent reacting flows. It assumes that reaction occurs in small turbulent structures, called fine scales. These small scale structures can be captured as a part of the cell, where Kolmogoroff-sized eddies containing combustion species are situated so close together that mixing on the molecular level is taking place. The EDC model evaluates the volume of each cell, where mixing on a molecular scale occurs and treats this part of the cell as a PSR.

The key reactive flow modelling issue is the calculation of source terms in reactive species transport equations, which are the average values of strongly non-linear reaction rates. Early models, dedicated for combustion applications, have been derived on the assumption of chemical equilibrium. Taking into account detailed kinetics of reactions results in much higher computational effort.

In the present work Eddy Dissipation Concept (EDC) (Magnussen, 1981) was used as a general concept for treating interaction between turbulence and chemistry. All reactions of the reactive components are assumed to react only in these spaces which are locally treated as a Perfectly Stirred Reactors (PSR) with a residence time:

$$\tau^* = 0.41 \cdot \sqrt{\frac{\nu}{\varepsilon}} \quad (1)$$

where ν is the kinematic viscosity, ε denotes turbulent kinetic energy dissipation rate. These parameters are calculated from turbulence model. Mass fraction occupied by fine structures is modeled as:

$$\gamma^* = [2.13 \cdot (\frac{\nu\varepsilon}{k^2})^{0.25}]^2 \quad (2)$$

The reaction rates of all species are calculated on a mass balance for the fine structure reactor. Denoting quantities with asterisk, the conservation equation of species i can be defined:

$$\frac{\rho^*}{\tau^*(1-\gamma^*)} (m_i^* - \overline{m}_i) = M_i \cdot \overline{\omega}_i^* \quad (3)$$

The mean net mass transfer rate of species i between the fine structures and the surrounding fluid can be expressed as:

$$R_i = \frac{\overline{\rho}\gamma^*}{\tau^*(1-\gamma^*)} (\overline{m}_i - m_i^*) \quad (4)$$

The EDC model is implemented into CFD code by solving the non-linear system of equations for the fine structure reactor in each control volume and finding R_i , which is the source term in species i transport equation.

3.3. NO oxidation mechanism

In most engineering cases implementation of a detailed reaction mechanism into CFD codes is not recommended due to large computational effort. For many purposes the required information can often be obtained with a less complete chemistry description. CFD simulations most often use simplified global reaction mechanism.

Appropriate reaction selection is crucial in terms of reliance on calculated results. The reactions between O₃ and NO_x include ozone decomposition as well as the reactions between O₃ and NO and subsequent conversion of intermediate nitrogenous species. Elemental reaction rates can be obtained from the National Institute for Standards and Technology (NIST) (NIST, 2012) kinetic database or GRI-Mech 3.0 (GRI-Mech, 2012).

Main reactions in ozone-nitrogen system are given in Table 2. Many others are possible but in terms of rate constants other reactions are less important (Wang et al., 2007). A global mechanism comprising of reactions 1 to 11 from Table 2 was verified in (Mok and Lee, 2006). The authors approximated the laboratory ozonizing chamber mixing ozone and flue gases with an ideal batch reactor model. A zero-dimensional algorithm was applied to solve the given global reaction mechanism. Concentrations of

NO, NO₂, NO₃, N₂O₅ and O₃ were calculated with varying concentrations of ozone added to the flue gas. The general trends of the calculated results agreed well with the experimental data.

The reaction of NO oxidation (1) is very fast. The forward and backward reactions (12, 13) are very fast as well, but the reaction product (N₂O₃) is unstable, and therefore ignored in most modeling studies (Jaroszyńska-Wolińska, 2002, Mok and Lee, 2006). However, N₂O₃ may play an important role in the absorption process (Głowiński et al., 2009) and for this reason it was included in the model.

Table 2. Global reaction mechanism of NO oxidation with O₃

1	NO + O ₃ → NO ₂ + O ₂	$k_1 = 2.59 \times 10^9 \exp(-3.176/RT)$
2	NO ₂ + O ₃ → NO ₃ + O ₂	$k_2 = 8.43 \times 10^7 \exp(-4.908/RT)$
3	NO ₂ + NO ₃ → N ₂ O ₅	$k_3 = 3.86 \times 10^8 T^{0.2}$
4	N ₂ O ₅ → NO ₂ + NO ₃	$k_4 = 6.93 \times 10^{15} \exp(-19.67/RT)$
5	NO + NO ₃ → 2NO ₂	$k_5 = 1.08 \times 10^{10} \exp(0.219/RT)$
6	NO + O → NO ₂	$k_6 = 3.27 \times 10^9 T^{0.3}$
7	NO ₂ + O → NO + O ₂	$k_7 = 3.92 \times 10^9 \exp(0.238/RT)$
8	O ₃ → O ₂ + O	$k_8 = 4.31 \times 10^{11} \exp(-22.201/RT)$
9	O + O ₃ → 2O ₂	$k_9 = 4.82 \times 10^{11} \exp(-4.094/RT)$
10	O + 2O ₂ → O ₃ + O ₂	$k_{10} = 1.15 \times 10^{11} T^{-1.2}$
11	O + O → O ₂	$k_{11} = 1.89 \times 10^7 \exp(1.788/RT)$
12	NO + NO ₂ → N ₂ O ₃	$k_{12} = 4.75 \times 10^9 (T/298)^{1.4}$
13	N ₂ O ₃ → NO + NO ₂	$k_{13} = 4.7 \times 10^{15} (T/298)^{0.4} \exp(-9.7/RT)$

4. RESULTS

The influence of ozone injection pattern (co-current and counter-current) and molar ratio *X* on the measured and computed mole fractions of NO and NO₂ in the reactor were compared. The obtained results were presented in form of axial profiles of mole fractions.

4.1. Co-current ozone injection

A comparison of the experimentally and numerically obtained axial profiles of the NO mole fraction for co-current ozone injection and the mole ratio *X* = 1.0 is given in Fig. 2. There is a substantial difference between both profiles because the experimental NO profile almost immediately dropped to zero and after about *L/D* = 15 settled to the level of about 20 ppm, while the numerically obtained NO graph decreased gradually along the reactor axis to finally approach the experimental NO profile.

The discrepancy visible in the first meter from the injection point can be explained by the turbulence-chemistry interaction. As noted in (Mok and Lee, 2006), where Perfectly Stirred Reactor experiment was considered, the longer residence times does not necessarily contribute towards larger NO conversion by ozone during the well-mixed process considered due to the net effect of faster reactions. It can be concluded that the process can be described as mixing-controlled not kinetically-controlled. The equilibrium conditions are rapidly achieved which is proved by experimental results.

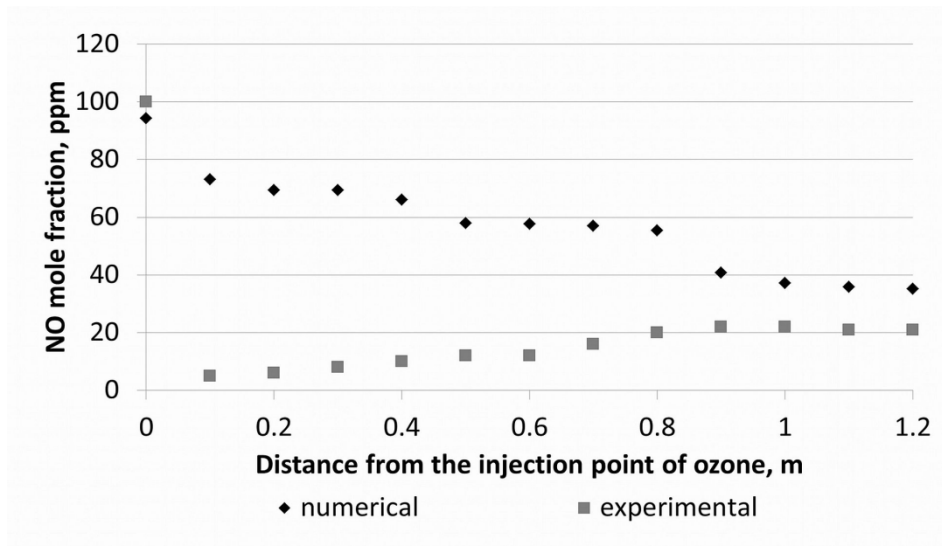


Fig. 2. Axial profiles of the numerically and experimentally determined NO mole fractions for co-current ozone injection and $X = 1.0$

Experimentally, in the region close to the nozzle, ozone could form a narrow jet. After some distance the flow is being turbulised and process of NO with O_3 mixing becomes intensified. The concentration of the O_3 is characterised by a very high gradient: a very high local concentration somewhere close to symmetry axis and very low concentration in the rest of the cross-section. In a distance from the nozzle due to turbulent the mixing of gases is more intensive so the experimental data are closer to numerical results.

The numerical calculations have over predicted mixing rate of ozone with NO close to injection location. Due to a very small injection diameter of ozone inlet, the nozzle in the carrier gas was simulated numerically as an additional source term in the control volume corresponding to the injection location. According to this approach mixing is more intensive close to ozone injection. It has to be noticed that perfect, computational conditions will never be reflected absolutely in the experiment.

Additionally, the visible differences close to the ozone injection show the limited applicability of proposed global reaction model implemented through Eddy Dissipation Concept under specific mixing conditions. Unfortunately, 11-step mechanism may produce inaccurate results in comparison to detailed one containing hundreds of reactions.

This interpretation was confirmed by the comparison of the calculated and measured profiles of the NO_2 mole fraction (Fig. 3). Up to about 0.2 m after the ozone injection the experimental NO_2 was close to null, because NO did not manage to deeply penetrate the reactor. After approximately $L/D = 15$ from the ozone injection location, the comparison of the calculated and measured profiles shows good agreement for the NO_2 mole fraction.

Better conformity between numerical simulation and the experimentally determined axial profiles of the NO mole fractions was achieved for $X = 1.5$ (Fig. 4). Both profiles approached each other after a shorter distance from the ozone injection side $L/D \approx 5$.

The experimentally and numerically obtained profiles of the NO_2 mole fraction are also demonstrated for $X = 1.5$, and after about $L/D = 10$ were similar to $X = 1.0$ (Fig. 5).

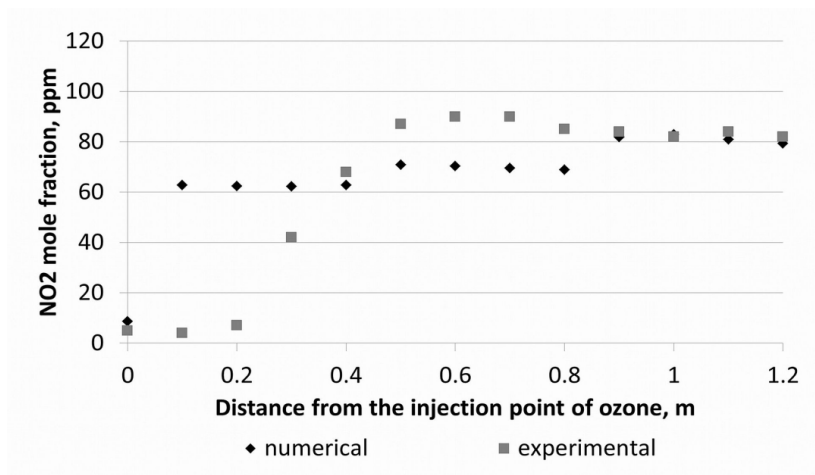


Fig. 3. Axial profiles of the numerically and experimentally determined NO₂ mole fractions for co-current ozone injection and $X = 1.0$

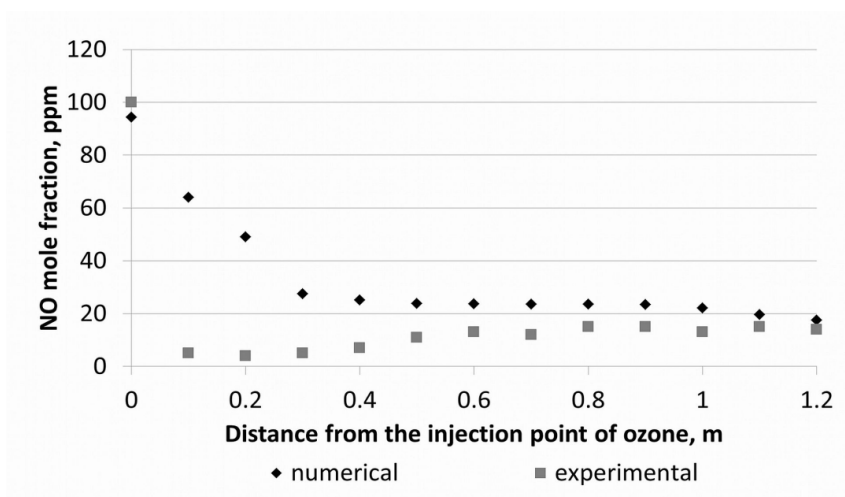


Fig. 4. Axial profiles of the numerically and experimentally determined NO mole fractions for co-current ozone injection and $X = 1.5$

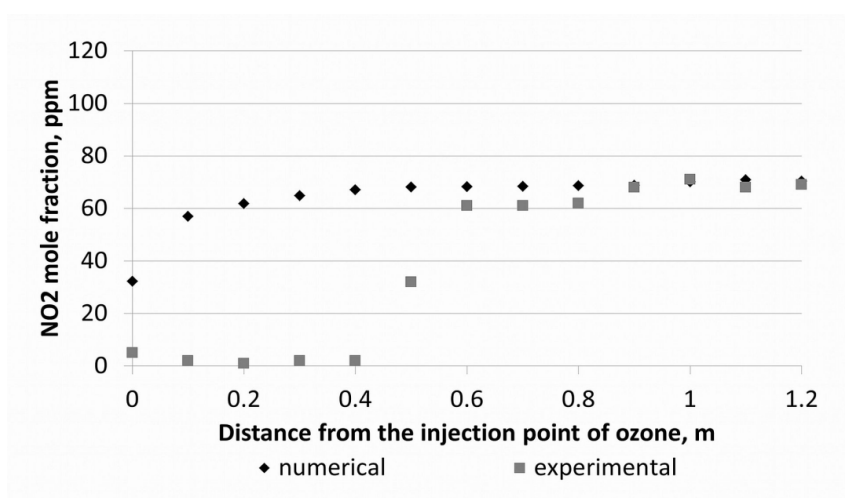


Fig. 5. Axial profiles of the numerically and experimentally determined NO₂ mole fraction for co-current ozone injection and $X = 1.5$

4.2. Counter-current ozone injection

The counter-current injection of ozone into the flow reactor ensured much faster mixing with NO in the carrier gas than it was the case for the co-current injection, which reduced the time required for NO ozonisation along the axis. In this case the profiles of NO and NO_2 mole fractions were stabilised just after $L/D = 2$ from the injection side (Fig. 6, 7), while for co-current injection over 4 times longer distance was needed.

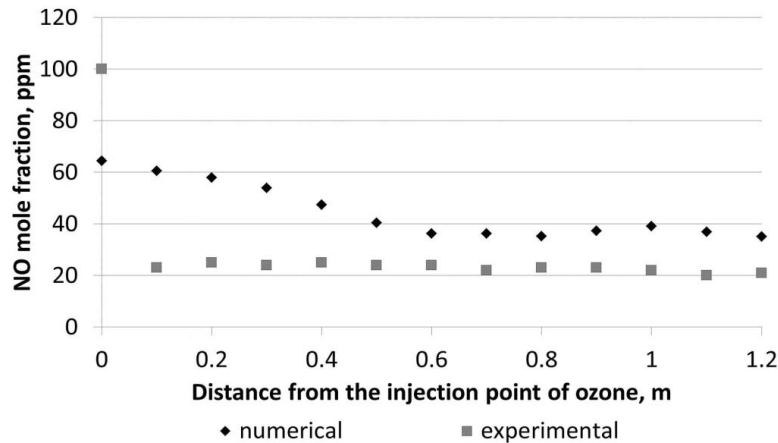


Fig. 6. Axial profiles of the numerically and experimentally determined NO mole fractions for counter-current ozone injection and $X = 1.0$

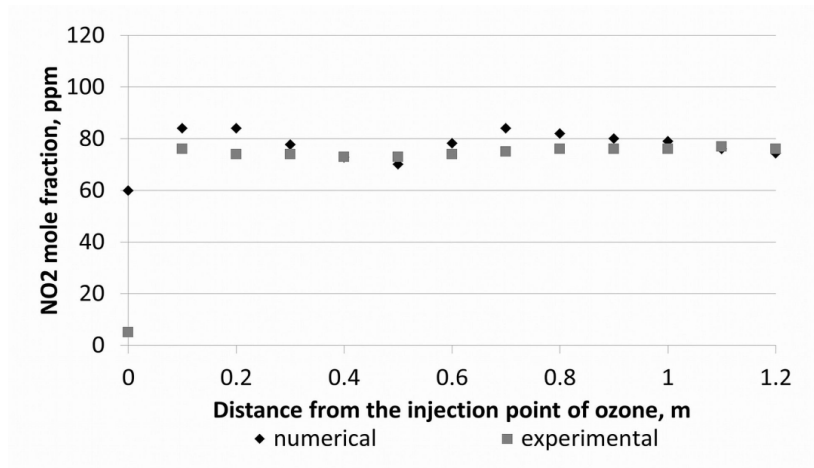


Fig. 7. Axial profiles of the numerically and experimentally determined NO_2 mole fractions for counter-current ozone injection and $X = 1.0$

It can be concluded that in case of counter-current injection the mixing rate was slightly under predicted by the model. That is why it takes a longer distance for calculated NO mole fractions to flatten. However, at the reactor end the experimentally and numerically obtained profiles of the NO mole fraction were settled close to each other.

For the stoichiometric molar ratio of NO and ozone streams ($X = 1.0$) entering the flow reactor, the outlet mole fraction of NO was settled at the approximate level of 30 ppm. A possible explanation of incomplete oxidation of NO could be the imperfection of NO/O_3 mixing: some amount of ozone could be lost in reactions with water vapor or solid impurities.

For the counter-current ozone injection after $L = 0.2$ m the results of numerical simulation were almost in perfect agreement with the experimental data for the NO_2 mole fraction (Fig. 7). A visible difference appeared only for the first measurement location (the nearest to the ozone injection point).

The results of the experimental investigations and the numerical calculations for the molar ratio of $X = 1.5$ were qualitatively and quantitatively very similar to the results obtained for the stoichiometric conditions ($X = 1.0$).

Although ozone was injected with a considerable excess ($X = 1.5$), nitric oxide NO was not completely oxidised at the reactor end. This phenomenon concerns both: the numerical and experimental data. The effect of incomplete NO oxidation at overstoichiometric conditions was also observed in earlier studies with Perfectly Stirred Reactor (Mok and Lee, 2006). Because of ozone excess and counter-current injection, imperfect mixing should not be the reason. Reactions (7) and (13) can be a possible source of residuary NO. Due to dissociation of ozone, excess oxygen radicals were generated and NO was produced in reaction (7). An extremely unstable N_2O_3 could also be a source of a secondary NO in reaction (13).

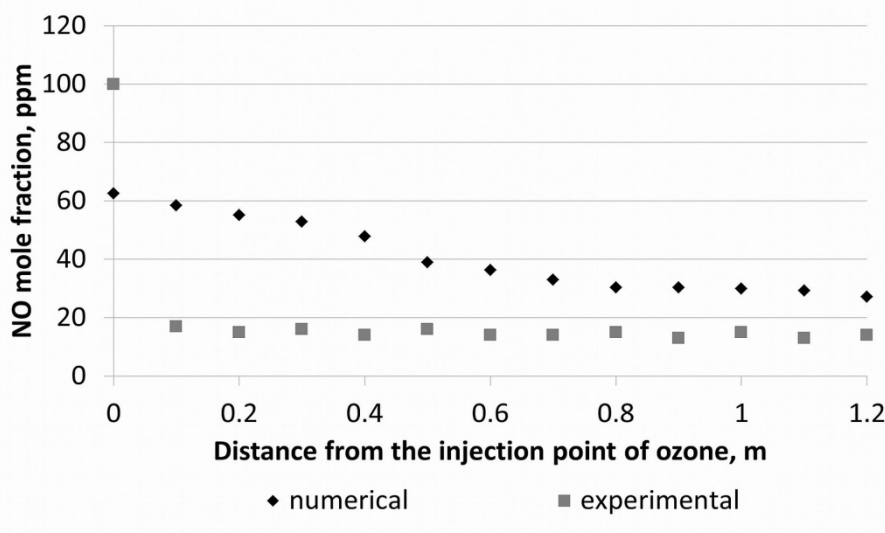


Fig. 8. Axial profiles of the numerically and experimentally determined NO mole fractions for counter-current ozone injection and $X = 1.5$

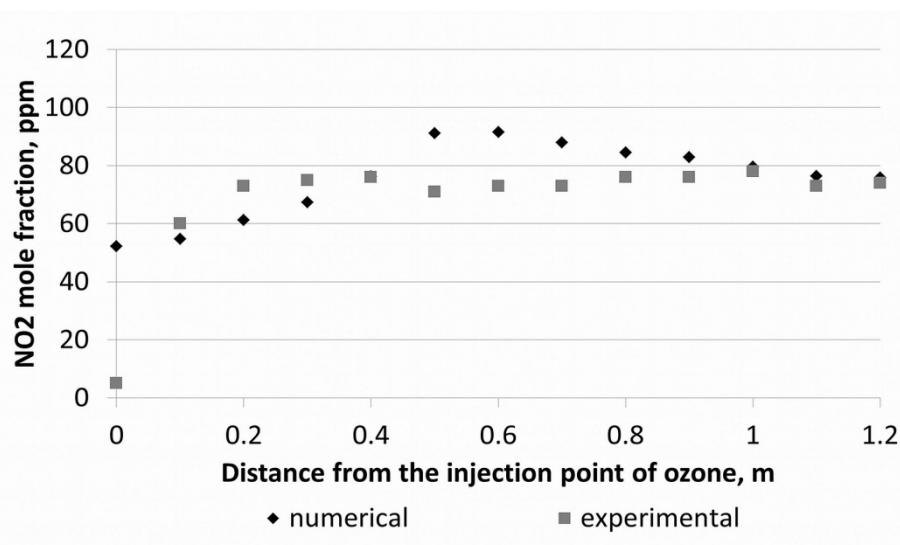


Fig. 9. Axial profiles of the numerically and experimentally determined NO_2 mole fractions for counter-current ozone injection and $X = 1.5$

Generally, due to faster mixing rates for counter-current ozone injection the occurring discrepancy between the measured and calculated profiles was smaller in comparison to co-current injection mode. Considerable differences between both values were observed only for the measurement sites near the ozone injection point ($L \leq 0.4$ m).

5. CONCLUSIONS

The analysis of the obtained results from the conducted studies leads to the following conclusions:

- It is possible to apply a simplified global homogeneous reaction mechanism of NO ozonisation into reactive turbulent flow simulation via EDC model (Magnussen, 1981).
- The quantitative conformity was not completely satisfying for all examined cases, but the final effect of NO oxidation was predicted correctly at the reactor outlet.
- The discrepancies close to the injection point can be explained by the turbulence-chemistry interaction and by relative simplicity of the global mechanism employed in the whole domain.
- The ozone injection nozzle was simulated numerically as an additional source term. In co-current case, the model over-predicts mixing close to the nozzle (in an experiment O_3 jet is formed along the axis), whereas mixing is under predicted in counter-current case.
- The process of NO conversion can therefore be described as mixing-controlled rather than kinetically-controlled.
- Both experiment and calculations show incomplete NO oxidation.
- Imperfect mixing may not be the only reason for incomplete NO oxidation. Due to dissociation of the ozone, excess oxygen radicals were generated and NO was produced in reaction (7) (Table 2). An extremely unstable N_2O_3 could also be a source of a secondary NO in reaction (13).

The results presented in the paper were obtained from research work co-financed by the National Centre of Research and Development in the framework of Contract SP/E/1/67484/10 Strategic Research Program – Advanced technologies for obtaining energy: Development of a technology for highly efficient zero-emission coal-fired power units integrated with CO_2 capture.

SYMBOLS

D	diameter, m
k	chemical reaction rate constant, L/mol/s
k	turbulent kinetic energy, m^2/s^2
L	length, m
m	mass fraction
M	molar mass, kg/kmol
R	mass exchange coefficient, $kg/m^3/s$
R	universal gas constant, J/K/mol
T	temperature, K
X	initial molar flux ratio of O_3/NO

Greek symbols

ε	dissipation rate of turbulent kinetic energy, ($kg/m/s^4$)
ρ	density (kg/m^3)

ν	kinematic viscosity (m^2/s)
ω^*	mean specie chemical reaction rate ($\text{kmol}/\text{m}^3/\text{s}$)

Subscripts

1 to 13	denotes reactions 1 to 13
i	denotes species i

REFERENCES

- Chironna R.J., Altshuler B., 1999. *Chemical aspects of NO_x scrubbing*. *Pollut. Eng.*, 31, 32-36.
- Cooper C.D., Alley F.C., 1994. *Air Pollution Control*. 2nd edR, Waveland Press, Inc., Long Grove, Illinois.
- Dora J., Gostomeczyk M.A., Jakubiak M., Kordylewski W., Mista W., Tkaczuk M. 2009. Parametric studies of the effectiveness of oxidation of NO by ozone. *Chem. Process Eng.*, 30, 621–634.
- Ellison W., 2003. Chemical process design alternatives to gain simultaneous removal in scrubbers, *POWER-GEN International*. Las Vegas, USA, 9-11 December 2003.
- Głowiński J., Biskupski A., Słonka T., Tylus W., 2009. Absorption of nitrogen oxides at the final stage of ammonium nitrite production. *Chem. Process Eng.*, 30, 217-229.
- GRI-Mech, 2012. <http://www.me.berkeley.edu/gri-mech/>
- Jakubiak M., Kordylewski W., 2010. Effectiveness of NO_x removal from gas via preoxidation of NO with ozone and absorption in alkaline solutions. *Chem. Process Eng.*, 31, 699-709.
- Jakubiak M., Kordylewski W., 2012. Pilot-scale studies on NO_x removal from flue gas via NO ozonation and absorption into NaOH solution. *Chem. Process Eng.*, 32, 229-239. DOI: 10.2478/v10176-012-0031-0.
- Jakubiak M., Kordylewski W., 2011. The effect of ozone feeding mode on the effectiveness of NO oxidation. *Chem. Process Eng.*, 32, 229-239. DOI: 10.2478/v10176-011-0018-2.
- Jaroszyńska-Wolińska J., 2002. Ozone application to a two-stage NO removal from waste gases. *Pol. J. Chem. Technol.* 4, 5-7.
- Jaroszyńska-Wolińska J., 2009. *Study of the reaction of nitrogen oxides with ozone generated in low-temperature plasma*. Institute of Nuclear Chemistry And Technology, Warsaw, Poland (in Polish).
- Kee R.J, Coltrin M.E., Glarborg P., 2003. *Chemically reacting flow. Theory and practice*. John Wiley & Sons, Inc., Hoboken, New Jersey.
- Launder B.E., Spalding D.B., 1974. The numerical computation of turbulent flows. *Comp. Meth. Appl. Mech. Eng.*, 3, 269–289. 1974. DOI: 10.1016/0045-7825(74)90029-2.
- Launder B.E., Reece G.J., Rodi W., 1975. Progress in the development of a Reynolds-stress turbulence closure. *J. Fluid Mech.*, 68, 537-566. DOI: 10.1017/S0022112075001814.
- Magnussen B.F., 1981. On the structure of turbulence and a generalized eddy dissipation concept for chemical reaction in turbulent flow. *Nineteenth AIAA Meeting*, St. Louis.
- Mok Y.S., Lee H., 2006. Removal of sulfur dioxide and nitrogen oxides by using ozone injection and absorption reduction technique. *Fuel Process. Technol.*, 87, 591-597. DOI: 10.1016/j.fuproc.2005.10.007.
- Nelo S.K., Leskela K.M., Sohlo J.J.K., 1997. Simultaneous oxidation of nitrogen oxide and sulfur dioxide with ozone and hydrogen peroxide. *Chem. Eng. Technol.*, 20, 40-42. DOI: 10.1002/ceat.270200108.
- NIST, 2012. Chemical Kinetics Database, <http://kinetics.nist.gov/kinetics/>.
- Prather M.J., Logan J.A., 1994. Combustion's impact on the global atmosphere. 25th *Symposium. (International) on Combustion*. Pittsburgh, USA, 31 July – 5 August 1994, 1513-1527.
- Puri I.K., 1995. The removal of NO by low-temperature O₃ oxidation. *Combust. Flame*, 102, 512-518. DOI: 10.1016/0010-2180(95)00042-5.
- Skalska K., Miller J.S., Ledakowicz S., 2011a. Effectiveness of nitric oxide ozonation. *Chem. Pap.*, 65, 193-197. DOI: 10.2478/s11696-010-0082-y.
- Skalska K., Miller J.S., Ledakowicz S., 2011b. Kinetic model of NO_x ozonation and its experimental verification. *Chem. Eng. Sci.*, 66, 3386-3391. DOI: 10.1016/j.ces.2011.01.028.
- Smoot L.D., 1993. *Fundamentals in coal combustion for clean and efficient use*. Elsevier, New York.
- Spalding D.B., 1976. Development of the eddy-break-up model of turbulent combustion. *Proc. Combust. Inst.* 16, 1657–1663.

- Van Doormaal J.P., Raithby G.D., 1984. Enhancements of the SIMPLE methods for predicting incompressible fluid flows. *Num. Heat Transfer*, 7, 147-163 DOI: 10.1080/01495728408961817.
- Wang Z., Zhou J., Fan J., Cen K., 2006. Direct numerical simulation of ozone injection technology for NO_x control in flue gas. *Energy Fuel.*, 20, 2432-2438. DOI: 10.1021/ef0603176.
- Wang Z., Zhou J., Zhu Y., Wen Z., Liu J., Cen K., 2007. Simultaneous removal of NO_x, SO₂ and Hg in nitrogen flow in a narrow reactor by ozone injection: Experimental results. *Fuel Process. Technol.*, 88, 817-823. DOI: 10.1016/j.fuproc.2007.04.001.
- Warnatz J., Maas U., Dibble R., 2006. *Combustion. Physical and chemical fundamentals, modeling and simulation, experiments, pollutant formation.*, 4th ed., Springer.

Received 1 August 2012

Received in revised form 08 May 2013

Accepted 21 May 2013